Materials Science and Engineering A 499 (2009) 106–110

Contents lists available at ScienceDirect

Materials Science and Engineering A

journal homepage: www.elsevier.com/locate/msea

Investigation on TIG welding of SiCp-reinforced aluminum–matrix composite using mixed shielding gas and Al–Si filler

Wang Xi-he*, Niu Ji-tai, Guan Shao-kang, Wang Le-jun, Cheng Dong-feng

School of Materials Science and Engineering, Zhengzhou University, Zhengzhou 450002, PR China

ARTICLE INFO

Article history:
Received 18 May 2007
Received in revised form 21 June 2008
Accepted 2 July 2008

Keywords:
He–Ar mixed gas
SiCp reinforcement
Al matrix composite
TIG welding

ABSTRACT

Using He–Ar mixed gas as shielding gas, the tungsten inert gas (TIG) welding of SiCp/6061 Al composites was investigated without and with Al–Si filler. Welded joint with filler were submitted to tensile tests. The microstructure and fracture morphology of the joint were examined. The results show that adding 50 vol.% helium in shielding gas improves the arc stability, and seams with high-quality appearance are obtained when the Al–Si filler is added. In addition, the interface reaction between SiC and matrix is greatly suppressed when using Al–Si filler. The microstructure of the welded joint displays non-uniformity with many SiC particles distributing in the weld center. The average tensile strength of weld joints with Al–Si filler is 70% above that of the matrix composites under annealed condition.

1. Introduction

Aluminum–matrix composites have wide applications, e.g. in the aerospace and automobile industries, due to their high specific strength, rigidity, wear resistance and good dimensional stability compared with unreinforced alloys [1–4]. One of the aluminum–matrix composite families with higher potential application, thanks to their excellent specific properties and acceptable fabrication costs, is constituted of medium- or high-strength aluminum alloys (i.e. 2xxx and 6xxx series) reinforced with SiC particles [4]. However, its further application and development are faced with the problem of poor weldability, caused by the great difference between aluminum–matrix and reinforcement in physical and chemical properties [5].

In recent years, the results of much research work have been published proposing the application of solid-state bonding techniques (diffusion bonding, friction welding, etc.) to solve those problems [2,5]. The weldability of SiC particle-reinforced aluminum–matrix composites has been investigated in friction welding [6]. Both inertia friction welding and continuous-drive friction welding can produce high-quality joints with uniform microstructures and promising mechanical properties, which are to date regarded as the most promising joining techniques [2]. Diffusion welding has been studied widely, including solid-state diffusion welding without interlayer. Transient liquid-phase diffusion bonding has also been used to join SiC particle-reinforced aluminum–matrix composites, and the results were favorable [2–6].

Fusion welding is the most flexible and versatile welding technology. Extensive investigation on welding of SiC particle-reinforced aluminum–matrix composites with high-power laser beam and electron beam has been conducted [7,8] in order to produce ideal microstructure and joint strength. However, the typical limitations of the procedures mentioned above as regards production capacity and equipment costs make it necessary to reconsider the possibility of the application of more productive welding processes [2]. Traditional tungsten inert gas (TIG) and metal inert gas welding techniques have been applied to join SiC particle-reinforced aluminum–matrix composites [2,9]. Their industrial application is much limited owing to the high viscosity of the molten pool, the segregation and agglomeration of reinforcing particles, and especially the serious interface reaction between SiC particle and aluminum–matrix, leading to less acceptable mechanical properties.

This paper describes an experimental research on the TIG weldability of SiC-reinforced 6061 aluminum alloy protected with helium–argon mixed gas.

2. Experimental procedures

Parent composite was a 6061 aluminum alloy reinforced with 15 vol.% SiC particles with an average size of 10 μm. Material which was produced by steer casting was received as a plate in annealed state after hot rolling forms with thickness of 3 mm. The tensile

* Corresponding author. Tel.: +86 371 63887501; fax: +86 371 63887508.
E-mail address: wangxihe@zzu.edu.cn (W. Xi-he).

0921-5093/$ – see front matter © 2008 Elsevier B.V. All rights reserved.
doi:10.1016/j.msea.2008.07.037

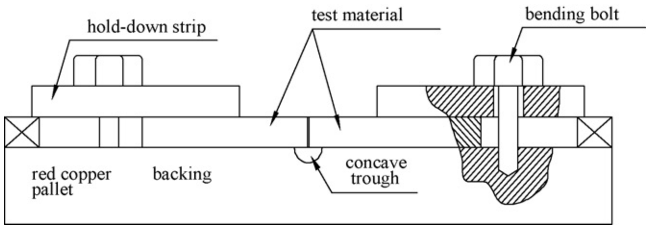

Fig. 1. Diagrammatic sketch of joint structure without groove.

Table 1
Composition of Al–Si alloy filler (wt.%)

Si	12.0
Mn	≤0.5
Fe	≤0.5
Mg	≤0.05
Ti	≤0.15
Ca	≤0.10
Cu + Zn	≤0.15
Al	Balance

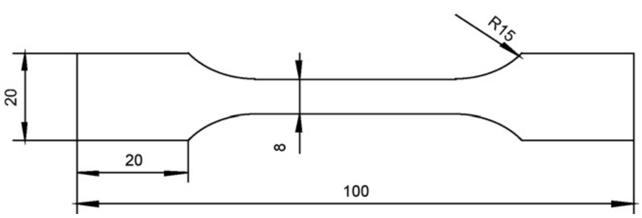

Fig. 2. Dimensions of tensile test specimen.

strength of the parent composite in annealed state is 271 MPa. For welding, the material was made into specimens with the dimensions of 60 mm × 30 mm × 3 mm by wire cutting. Prior to welding, the specimens were polished with abrasive paper and were thoroughly washed with acetone to clean greasy dirt and impurities.

The joint structure without groove was adopted in the welding process. As shown in Fig. 1, a hold-down strip was used to prevent the displacement of samples; the red copper pallet had the effect of accelerated cooling for the weld. The penetration rate and root shape of the seam were controlled by the concave trough in the pallet.

The specimens were welded applying single electric arc discharge on one face with filler of Al–Si alloy, using a multifunction TIG WSE-315 welding machine by manual welding. The composition of the filler metal is listed in Table 1. An AC square-wave current of about 60 A was adopted. The diameters of tungsten electrode and injecting nozzle were 2.5 mm and 7 mm, respectively. The electric arc was always generated in a mixture gas of helium and argon using a gas flow of 115 ml/s. The purities of helium and argon were 99.99%. The welding parameters were selected to achieve complete penetration of the molten pool through the specimen thickness. The welding speed (18 cm/min) and the arc length (4 mm) were constant for all the welding tests. The angle between the blowtorch, filler and specimens were in the ranges of 75–80° and 10–15°, respectively.

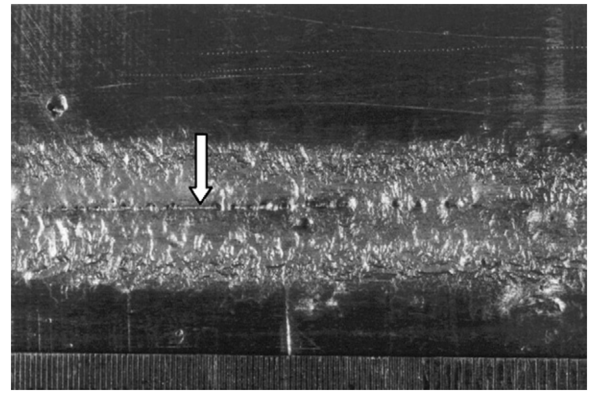

Fig. 4. Appearance of TIG welded joint without filler.

Both parent composites and welded ones were machined in the form of tensile test specimens as shown in Fig. 2. The tensile test of specimens was conducted on a universal testing machine at a nominal applied strain rate of 1.0 mm/min. The fracture surfaces were examined by scanning electron microscopy (SEM). The microstructure of the welded joint was examined by OLYMPUS optical microscopy.

3. Results and discussion

3.1. Effect of mixture ratio of helium and argon on electric arc characteristic

The mixture ratio of helium and argon was changed in the range of 0–100% to observe the electric arc shape and the shielding effect. The results show that the stability of the electric arc increases with the raising of helium in the gas flow. However, the stability of the electric arc decreases when the ratio of helium is higher than 60%, as shown in Fig. 3. At the same time, the mixed inert gas does not produce good protection for the composite due to the heavy spattering. It was found that the deepest penetration of specimen is obtained with 50 vol.% helium in the mixed gas, which was resulted from good clean up function of cathode, the stable inflammation and high temperature of arc.

Compared with air, the argon has played a good role of protection and stable electric arc in the welding process, owing to heavier

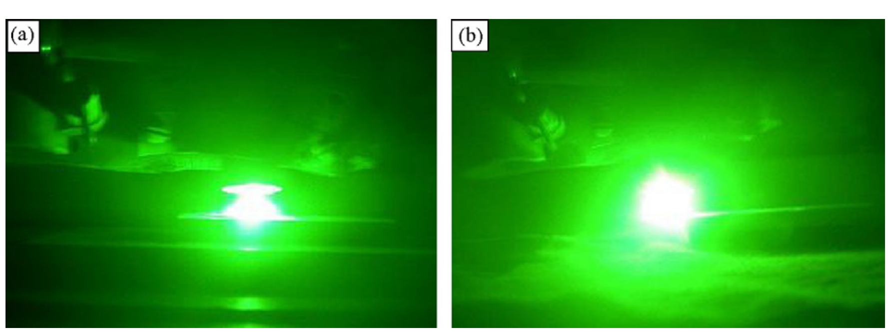

Fig. 3. Electric arc shape of 50% (a) and 60% (b) He in the mixed gas.

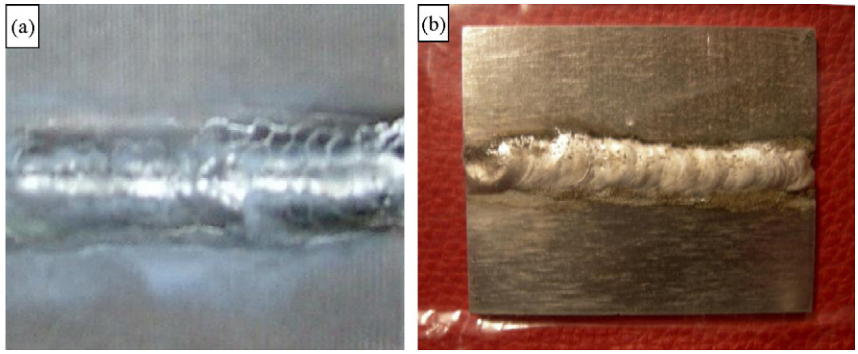

Fig. 5. Appearance of TIG weld joint with Al–Si filler: (a) Ar gas and (b) Ar–He mixed gas.

density, smaller heat capacity ratio and heat conductivity. In contrast to argon, the helium has higher ionization potential and heat conductivity. Under the same welding current and arc length, the helium has higher arc voltage and provides higher power. In addition, the higher energy density and focused arc column of helium arc result in a deeper penetration of weld. Therefore, adding of a doping helium gas in the shielding gas improves not only the arc stability but also provides the seams with high-quality appearance and prevents oxidation of the specimens and welding spatter on the specimens [10].

3.2. Formability of weld with and without Al–Si alloy filler

3.2.1. Without Al–Si alloy filler

Fig. 4 shows the appearance of TIG weld joint without filler using a shield gas of 50 vol.% helium. From Fig. 4, we can see that the abutting joint line (indicated by arrowhead) is clearly observed. The ripple appearance, often found in aluminum welding, did not form and bad semblance of welded seam was obtained. The fused slag and bulge are obviously seen on the seam surface. The reasons for these phenomena lie in the enormous difference in the phys-

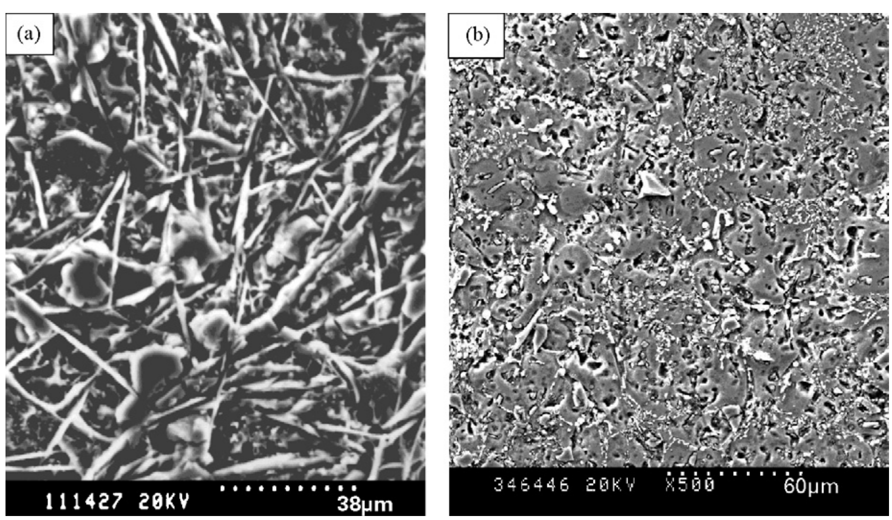

Fig. 6. Microstructure of TIG weld joint: (a) with and (b) without Al–Si filler.

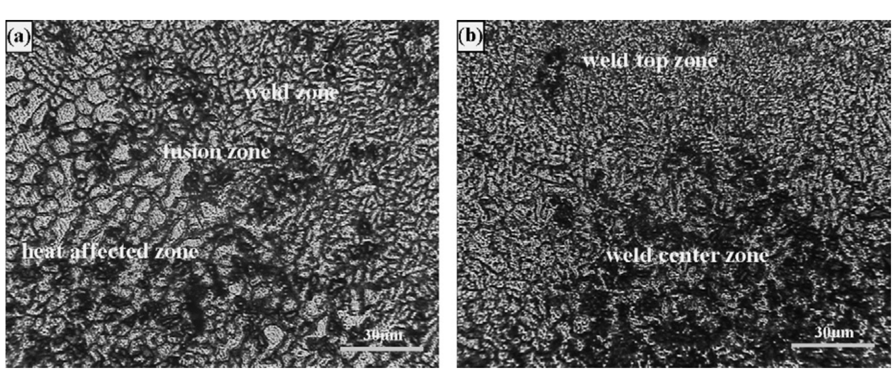

Fig. 7. Microstructures of welded joint with Al–Si filler.

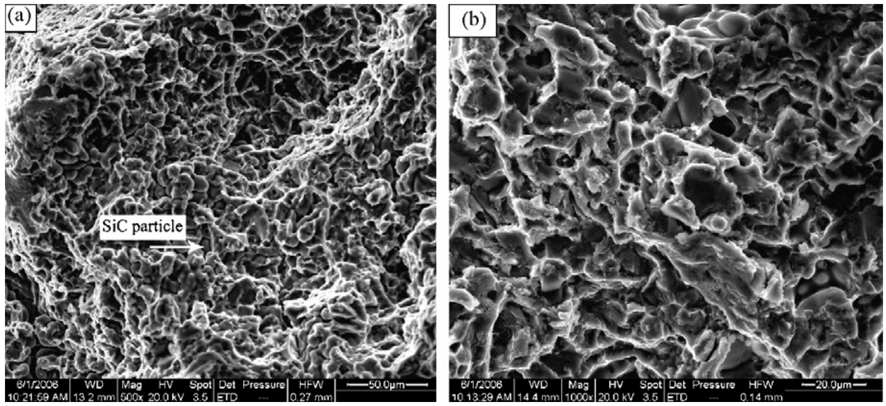

Fig. 8. Scanning electron fracture micrographs of tensile specimen for welded joint with Al–Si filler.

ical and chemical properties of SiC particles and aluminum alloy matrix.

It is well known from numerous previous studies [2,11] that when the molten aluminum–matrix comes into contact with the SiC particles during liquid-phase processing of aluminum (casting or welding), an interfacial reaction (seen in Eq. (1)) occurs between them to form an acicular aluminum carbide and free silicon:

$$4Al + 3SiC \rightarrow Al_4C_3 + 3Si \quad (1)$$

The reaction product Al_4C_3 is also unstable in wet environments because it undergoes rapid hydrolysis causing corrosion of the composite. Moreover, the other reaction product, Si, may generate Al–Si eutectic aggregates both in the particle/matrix interfaces and in the grain boundary matrix, decreasing the ductility of the composite [2]. The fused slag on the joint surface may be contributed to the intensive interface reaction between SiC particles and aluminum–matrix.

3.2.2. With Al–Si alloy filler

The Al–Si filler was used to improve the fluidity of the welding pool. Fig. 5 shows the weld appearance with Al–Si filler. Compared with Figs. 4 and 5, we can see that the weld formation with filler is evidently improved and the fish scale weld ripple forms. From Table 1, we know that the filler contains 12 wt.% Si. When the Al–Si filler was added into the molten pool, the Si content in the weld pool was obviously increased. Hence, the Gibbs free energy of Si was visibly increased and the harmful interface reaction was greatly depressed, due to the activity of Si being raised [12]. Moreover, the high Si content in the weld puddle resulted in the formation of Al–Si eutectic and the fluidity improvement of the liquid metal in fused bath. Therefore, the high-quality appearance was obtained when Al–Si filler added.

Fig. 5 also compares the appearance of welds with Ar gas and Ar–He mixed gas. It can be observed that the width of the weld using Ar–He mixed gas (Fig. 5(b)) is narrow than that with Ar only (Fig. 5(a)). It is attributing to the higher concentration of the arc with Ar–He mixed gas.

The microstructures of the joint are compared in Fig. 6. Fig. 6(a) demonstrates the acicular reaction product of Al_4C_3 in weld with Al–Si filler, however, in Fig. 6(b), the acicular Al_4C_3 have not been found in the weld without Al–Si filler. The result indicates that the addition of Al–Si filler is helpful to obtain a high-quality appearance and restrains the interface reaction between reinforcement and matrix. These experimental results are agreed with that in the literature [13], although the pulse TIG welding was used in it.

3.3. Microstructure and mechanical properties of welded joint with Al–Si filler

Fig. 7 shows the microstructures of the welded joint with Al–Si filler, including heat-affected zone, fusion area and weld zone. From the figure, it can be seen that no harmful needle-like Al_4C_3 is formed in the weld zone and in the vicinity of the weld junction. Moreover, the drawbacks, such as gas porosity and oxidation are barely seen. However, the microstructure of the weld joint is inhomogeneous, as shown in Fig. 7(b). Exquiaxed grains and many SiC particles are found in the weld center; columnar crystals and a lower number of SiC particles can be found in the bond zone. The microstructure in the weld top has few SiC particles and mainly consists of Al and Si, as shown in the top part of Fig. 7(b). In contrast, numerous SiC particles are found in the weld center, weld bottom and bond zone. The above results demonstrate that the distribution of the reinforcement phase in the three parts of the weld is inhomogeneous, resulting from the non-uniform composition in the fused bath.

The maximum tensile strength of the weld joints with Al–Si filler is 240 MPa. It is about 88% of the matrix composites under annealed condition and the average tensile strength of the three weld joints is about 70% of the matrix. The breaking points of the tensile test specimen mainly lie in the heat-affected zone.

Fig. 8 shows the fracture morphology of the tensile-tested specimens with high-quality welding joint. As shown in Fig. 8(b), it can be seen that almost all of the SiC particles are covered with a coating of aluminum–matrix, indicating the excellent interfacial bonding between SiC particles and matrix in the parent composites. Moreover, ductile regions with near-featureless non-circular dimples, called "tear ridges" and voids (Fig. 8(a) and (b)) were frequently observed. These are the signs of plastic deformation; therefore, the fracture mechanism of the investigated specimen with Al–Si filler mainly belongs to the ductile rupture.

4. Conclusions

(i) Adding of a doping helium gas in the shielding gas improves not only arc stability but also provides the seams with high-quality appearance.
(ii) Compared weld formability of composites with and without Al–Si filler, the high-quality appearance welded seam is obtained when the Al–Si filler added. In addition, the harmful interface reaction between SiC particles and aluminum–matrix is greatly depressed. However, the microstructure of the welding joint has evident non-uniformity.

(iii) The maximum tensile strength of the welded joints with Al–Si filler is about 88% and the average value is 70% of that for the matrix composites under annealed condition. The fracture mechanism of the said specimen with Al–Si filler mainly belongs to the ductile rupture.

Acknowledgement

Thanks to the financial support of the national high-tech research and development program of China (863 program) (Project No. 2006AA03Z568) for the work present here.

References

[1] M.B.D. Ellis, Int. Mater. Rev. 41 (1996) 41–58.
[2] A. Ureña, M.D. Escalera, L. Gil, Compos. Sci. Technol. 60 (2000) 613–622.
[3] J.M. Torralba, C.E. Da Costa, F. Velasco, J. Mater. Process. Technol. 133 (2003) 203–206.
[4] L. Ceschini, I. Boromei, G. Minak, A. Morri, F. Tarterini, Compos. Part A: Appl. Sci. Manuf. 38 (2007) 1200–1210.
[5] J.T. Niu, D.K. Zhang, G.J. JI, Trans. Nonferr. Met. Soc. China 13 (2003) 289–293.
[6] O.T. Midling, O. Grong, Acta Metall. Mater. 42 (1994) 1595–1609.
[7] D.K. Zhang, Y.B. Chen, J.T. Niu, China Weld. (in Chinese) 10 (2) (2000) 140–144.
[8] Y.L. Chen, L.G. Yu, Proceedings of SPIE2 of the International Society for Optical Engineering High Power Lasers in Manufacturing [C], New York, USA, 2000, pp. 143–146.
[9] G.J. Ji, J.G. Xie, W.T. Xue, J.T. Niu, Nonferr. Met. (in Chinese) 55 (2003) 1–4.
[10] T. Ernst Mikols, U. Burkhard Haas, United States Patent, Patent No. US6991748B2, 2006.
[11] D.S. Shin, J.C. Lee, E.P. Yoon, H.I. Lee, Mater. Res. Bull. 32 (1997) 1155–1163.
[12] G.J. Ji, J.G. Xie, W.T. Xue, Nonferr. Met. (in Chinese) 55 (2003) 21–23.
[13] M.A. Chen, C.S. WU, J.Q. Gao, Trans. Nonferr. Met. Soc. China 12 (2002) 805–810.